Landslides: Evaluation and Stabilization, Lacerda, Ehrlich, Fontoura & Sayão (eds)
© 2004 Taylor & Francis Group, London, ISBN 04 1535 665 2

Numerical modelling of the run-out of a muddy debris-flow. The effect of rheology on velocity and deposit thickness along the run-out track

Th.W.J. Van Asch
Utrecht Center of the Environment and Landscape Dynamics, Utrecht, The Netherlands

J.-P. Malet, A. Remaître & O. Maquaire
Institut de Physique du Globe, UMR 7516 CNRS-ULP, Strasbourg, France

ABSTRACT: With a simple numerical model the effects of yield strength and pore pressure characteristics on the run-out characteristics of a small muddy debris-flow were analyzed. The muddy debris-flow was initiated in a secondary scarp of the Super-Sauze earthflow (Alpes-de-Haute-Provence, France). Assuming a purely cohesive material, model predictions of the run-out time and distance, and the uniform distribution of deposit thickness along the track were in good accordance with those measured in the field. Simulations showed that when assuming a more frictional character of the material clear concentration of material occurred at the flattening parts of the slope track.

1 INTRODUCTION

Clayey flow-like landslides are characterized by their capability to suddenly change behaviour. Landslides on black marl slopes of the French Alps are in most cases complex catastrophic failures in which the initial structural slides transform into slow-moving earthflows. Under specific hydrogeological conditions, these earthflows can transform into induced debris-flows. Due to their sediment volume, and their high mobility, debris-flow induced by such landslides are very dangerous. It is therefore important to understand why and how some landslides transform into debris-flow while most of them stabilize and to analyze their rheological and hydrological behaviour, which determine the run-out characteristics (Ancey, 2001).

Run-out distances of debris-flows are among others strongly controlled by the rheological behavior of the material. Several rheological models are currently applied to model one-phase constant-density debris-flows. The Bingham model assumes a constant yield strength, which is attributed to the undrained cohesive strength (c) of the material. In that case the yield strength is independent of the normal stress to the base of the flow and hence the flow thickness (Coussot, 1997). In the Coulomb-viscous model, the yield strength is linearly related to the normal stress. In that case the material is a pure ($c = 0$) frictional (ϕ-) material. According to Johnson & Rodine (1984) the yield strength can also contain both a cohesion and frictional component.

It is important to know for estimating run-out distances, whether the material has frictional character or cohesive character. In the first case only slope angle determines where the debris-flow will stop. In the second case both flow depth and slope angle are the limiting factors. On a flattening slope track, frictional material will stop at a certain threshold gradient, irrespective of the thickness of the flow, while purely cohesive material can continue its way down slope when the cohesive (constant) yield strength is still relatively low compared to the total driving force, which is determined by the flow depth.

Another important factor is the effect of pore pressure on run-out characteristics. During run-out, pore pressure can be considered as a constant value. However excess pore pressure may be generated during initial failure, which will dissipate during the run-out process (Major & Iverson, 1999, Major, 2000, Iverson, 2003).

The aim of this paper is to analyze with a simple numerical model the effect of yield strength and pore pressure characteristics on the run-out characteristics of muddy debris-flows. The model was tested on

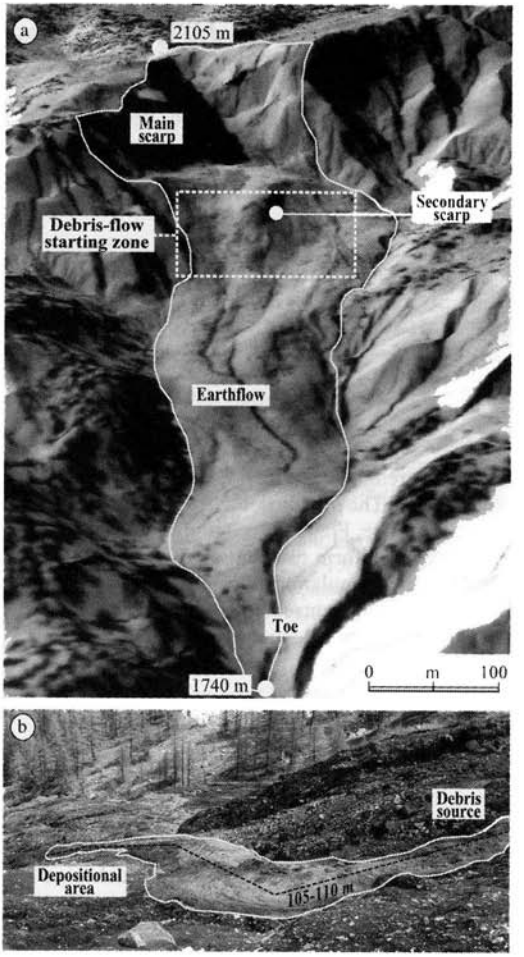

Figure 1. Aerial ortho-photograph of the Super-Sauze earthflow (a) and morphology of a small muddy-debris flow released in 1999 from the secondary scarp (b).

a small debris-flow, which was initiated by a slump in a secondary scarp of the Super-Sauze earthflow (Fig. 1a).

2 DESCRIPTION OF THE FLOW

The Super-Sauze earthflow affects the north-facing slope of Ubaye valley (Alpes-de-Haute-Provence, South French Alps), where the combination of steep slopes (up to 35°), downslope stratigraphic dip and the lack of vegetation make this basin one of the most active landslide, flow and debris-flow prone areas (Maquaire et al., 2003).

The clayey slow-moving earthflow (0.01 to 0.40 m.day^{-1}) is characterized by a complex style of activity because of its capability to suddenly change behaviour. It can transform into a muddy debris-flow characterized by high velocities (1 m.min^{-1} to 1 m.s^{-1}) and run-out distances. A dozen of events were observed and the geometry and morphology of the run-out tracks and deposition zones were carefully mapped (Malet, 2003).

Malet et al. (in press) have stressed that these muddy debris-flows, initiated in an impermeable clayey material, occur through a combination of heavy and sustained rainfalls, thawing soils and snowmelt.

It is important to notice that at this date, only small volume events were released (500–8000 m^3) from the earthflow (750,000 m^3). Nevertheless, morphological evidences and numerical simulations prove that the release of larger volumes is a realistic option for specific climatic and hydrogeological circumstances. Therefore, the main objective is to propose a numerical model for the runout of these debris-flows.

The model described below is calibrated, in a first stage, on a very small event which has occurred on 1999, May 5th (Fig. 1b). A volume of 100 m^3 failed suddenly from the secondary scarp of the earthflow, flowed rapidly on the hillslope in the first 30 min until a distance of 50 m from the slumping point, and then continued flowing at a slower velocity during 60 min. The final run-out distance reached 105 m from the source area.

In the depositional area, the thickness of the deposits reaches 0.20 to 0.25 m whilst only 0.05 to 0.15 m in the run-out track. Deposits are mainly heterometric lateral levees and small accumulation lobes. These lobes are flat, with convex sides and are hardly cemented to the surface. The cross-section of the levees reveals a curved profile, and the levees of the dried deposits are characterized by strong cohesion. Furthermore, due to the specific morphological conditions, most of the materials involved came to a stop on the flattening areas of the slope gradient.

The peak velocity, estimated by the Johnson method (Johnson & Rodine, 1984; Hungr et al., 1984) has reached 2.1 m.min^{-1} in the upstream part of the run-out track, and 1.2 m.min^{-1} in the downstream part.

3 DESCRIPTION OF THE MODEL

The constitutive equation used in the model is a simplified 2-parameters Bingham plastic rheology described mathematically as follows in a simple shear geometry (Bingham, 1922):

$$\frac{\partial v}{\partial y} = \frac{1}{\eta}(\tau - \tau_0) \qquad (1)$$

where v = velocity (m.s^{-1}); y = depth perpendicular to the velocity; η = dynamic viscosity (kPa.s);

τ = shear stress (kPa); τ_0 = yield strength (kPa). Bingham plastic fluids exhibit a linear shear-stress shear-rate behavior after an initial shear-stress threshold has been reached (Ancey, 2001). In the first development of the model, the more accurate 3-parameters non-linear Herschel-Bulkley viscoplastic rheology has not been tested (Coussot, 1997).

Since the debris-flow has a changing geometry, inter slice forces are not symmetrical like in the infinite slope model. Therefore the shear stress and yield strength in equation (1) are calculated with the simplified Janbu equilibrium model (Janbu, 1954, Nash, 1987):

$$F^t = \frac{\sum \left[c' L + \left(W' - (U'_{normal} + U^{t-1}_{excess}) \right) \tan \phi' \right] / n_\alpha}{\sum W' \tan \alpha} = \left(\frac{\sum S}{\sum T} \right) \quad (2a)$$

$$n_\alpha = \cos^2 \alpha \left(1 + \tan \alpha \frac{\tan \phi'}{F^{t-1}} \right) \quad (2b)$$

where W = weight of an individual slice j (kN); U = pore water force on the slip surface of slice j (kN); c' = cohesion (kPa); ϕ' = effective friction angle (°); α = slope angle of slice j (°); L = length of the slip surface of slice j (m); $S = \tau_0 L$ is the resisting force of slice j (kN); $T = \tau L$ is the mobilized shearing force of slice j (kN). This stability model satisfies force equilibrium on each slice and moment equilibrium on the whole failure surface (Duncan & Wright, 1980).

In the presented simulation, the width of the slices is 10 m while the first 5 slices in the source area have a width of 5 m. The Janbu equation delivers the yield strength and the shear stress, which are needed for equation (1). Equation (2a) contains F on both sides, which is solved iteratively in the first time step. In the following time steps F^t on the left side of equation (2a) is calculated with F^{t-1} obtained from the former time step and which is substituted for each slice in equation (2b) to calculate the right side of equation (2a). Assuming a velocity profile, which increases linearly with flow depth, the displacement of mass in $m^3.m^{-1}$ per times step is given by:

$$q = \tfrac{1}{2} v \Delta t \left(h_p + h_j \right) \quad (3)$$

where v = velocity, Δt = time step (5 seconds in our simulations); h_p = thickness of the rigid plug (m); h_j = total depth of the slice j (m).

The thickness of the rigid plug is given by:

$$h_p = \frac{c L h_j}{T - N' \tan \phi'} \quad (4)$$

3.1 N′ is obtained by resolving the forces per slice vertically:

$$N' = W / \cos\alpha - U - T \tan\alpha \quad (5)$$

The routing of the material in a time step is done by a simple mass balance equation:

$$\Delta q_j = q_{j-1} - q_j \quad (6)$$

where the slice j–1 lies upstream of slice j. A zero ϕ-value in equation (2) delivers a Bingham behavior of the material. For the Coulomb viscous flow behavior a combination of c- and ϕ-values (including a c = 0 condition) can be selected.

A pore pressure ratio p_u, defined by equation (7), is applied for each slice during the run-out:

$$p_u = \frac{h_w \gamma_w}{h_j \gamma_s} \quad (7)$$

where h_w = vertical height of the groundwater (m); γ_w = unit weight of water ($kN.m^{-3}$); γ_s = unit weight of saturated material ($kN.m^{-3}$). For a given p_u-value, a pore water force U can be calculated for equation 2a for each slice as follows:

$$U = p_u h_j \gamma_s L \quad (8)$$

During run-out, a constant pore pressure ratio or a dissipation of excess pore pressure can be assumed. Assuming that the muddy debris-flow is completely saturated ($h_w = h_j$ in equation 7) the amount of excess pore pressure in terms of the pore pressure ratio is:

$$p_u^{excess} = p_u - \frac{\gamma_w}{\gamma_s} \quad (9)$$

During run-out, dissipation of excess pore pressure is estimated by Therzaghi's theory of one-dimensional consolidation of an open layer (Whitlow, 1995). The fractional dissipation (F_r) of p_u-excess during an elapsed run-out time t = i is given by:

$$Fr^{t=i} = 1 - \frac{8}{\pi^2} \left[e^{-(\pi^2/4)T_v} + \frac{1}{9} e^{-(9\pi^2/4)T_v} + \frac{1}{25} e^{-(25\pi^2/4)T_v} \ldots \right] \quad (10)$$

where T_v = dimensionless time factor of one-dimensional consolidation and pore water dissipation process. F_r has a value between 0 and 1 (= complete dissipation of excess pore pressure).

T_v in equation (12) is defined as follows:

$$T_v = \frac{C_v t_i}{d^2} \quad (11)$$

where t_i = elapsed time (s); d = length of the drainage path that for an open layer equals half the mean thickness of the flow (m); C_v = coefficient of consolidation ($m^2.s^{-1}$).

For each time step the amount of excess pore pressure is calculated by equation (12):

$$p_u^{excess\ t=i} = p_u^{excess\ t=0} - Fr\, p_u^{excess\ t=0} \quad (12)$$

4 MODEL RESULTS

Based on field observations, the starting volume, released from a slumping block, was estimated at $15 m^3.m^{-1}$. The first set of simulations was carried out with a constant pressure ratio of $p_u = \gamma_s/\gamma_w$ assuming a completely saturated flow with no excess pore pressure. Calibrations were carried out on the run-out distance, which was 105–110 m from the source area and the run-out time, which was around 90 min. For each model run a ϕ-value was selected starting with $\phi = 0$ (Bingham behavior). The c and ϕ- values were obtained by calibration. The cohesion (c) could be calibrated on run-out distance, while the dynamic viscosity (η) could be calibrated on the run-out time.

For all ϕ-values between 0 and 26° a c-value and a η-value could be found, that fits the observed run-out distance and time. Table 1 and Figure 2 show three examples (scenario 1–3).

With increasing ϕ-values the dynamic viscosity decreases. This is explained by the overall increase in resistance of the flow due to the dependency of friction on flow depth. Therefore, in order to match the observed run-out time the dynamic viscosity has to be lowered. However the calibrated viscosities (η) are much higher than the viscosities measured in the laboratory with parallel-plates rheometrical tests and inclined-plane tests; the maximum viscosity is 0.2 kPa.s (Malet et al., 2003).

Table 1. Four scenarios (S1–4) with combinations of theological parameters fitting the observed run-out distance and run-out time of the small muddy debris-flow.

	ϕ (°)*	c (kPa)	η (kPa.s)	C_v ($m^2.s^{-1}$)
(S-1)	0*	0.72**	38.5**	n.a
(S-2)	18*	0.37**	20.5**	n.a
(S-3)	22*	0.25**	13.8**	n.a
(S-4)	30*	0*	14.0**	3.10^{-6}**

* Selected parameter. ** Calibrated parameter.

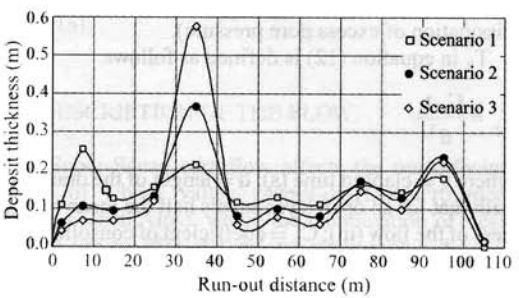

Figure 2. Run-out distances and distribution of deposit thickness along the track of the muddy debris-flow for scenario 1–3 given in Table 1.

Figure 2 shows that with increasing ϕ-values there is an increase in concentration of material deposition between 30 and 40 m and 90–100 m from the source area. These are the points where the debris-flow track shows a clear flattening of the slope gradient. The most regular distribution is obtained in the simulation for a $\phi = 0$ material (Fig. 1). The observed deposit thickness shows also a more regular distribution between the track, which varied between 0.15 and 0.25 m. It can therefore been hypothesized that the material has a dominant cohesive character.

The back-analyzed cohesion (Table 1) lies within the range of values measured in the laboratory (between 0.01 and 1 kPa, (Malet et al., 2002, 2003).

Differences in velocities were observed between materials with a different yield strength character. Figure 3 shows the change in velocity along the track during the run-out. Differences in velocity are remarkable at the steeper slope track during the first phase of the run-out process. This is explained by a difference in the calibrated dynamic viscosity (see above).

The question arises whether the observed more or less even distribution of material along the track can be simulated with a pure frictional material, which shows a decay of pore pressure during the run-out process. In the laboratory, triaxial tests were carried out on remolded samples (fine fraction <2 mm, Malet, 2003). Clearly no cohesion was present and the critical ϕ-values ranged between 26–30°.

These frictional values did not allow the material to pass the first flattening slope gradient at 30–40 m from the source area. Therefore a number of model runs were carried out where excess pore pressure during run-out was able to let the material pass the first threshold while, due to dissipation, it could stop at the second threshold near the observed final run-out distance. Since the muddy debris-flow was triggered by a slump failure, liquefying a part of the material, it is assumed that at the start of the run-out stage the material has a pore pressure ratio of $p_u = 1$. Based on the laboratory results, a pure frictional material of $\phi = 30°$ (c = 0) was used in the simulation. The model was

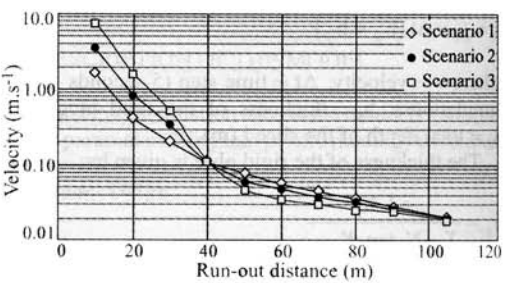

Figure 3. Differences in debris-flow front velocities along the track of the muddy debris-flow for scenario 1–3 given in Table 1.

calibrated again on run-out distance (105 m) and run-out time (90 min). Calibration was performed with the dynamic viscosity (η) and the coefficient of consolidation (C_v). A unique combination of η (14 kPa.s) and C_v (3.10^{-6} $m^2.s^{-1}$) was found, which fits the observed run-out distance and time (Table 1, Scenario 4).

Figure 4 shows the decrease in pore pressure ratio in combination with the position of the front. About half of the material is able to pass the first threshold. After 15 min, pore pressure has dropped down from 0.95 to 0.63 and the material is not able anymore to pass the first threshold. After 15 minutes there is only a slight accumulation of incoming upslope material.

Between 15 and 90 min, the debris-flow front moves slowly from 95 to 105 m The material is not able to pass this second threshold because of the lowered pore pressure but there is a clear accumulation of incoming upslope material.

The simulated profile of the debris-flow deposit shows a remarkable concentration of accumulated material at the first and second slope threshold, with a maximum thickness of respectively 0.6 and 0.4 m. In between these local slope thresholds the thickness of the deposit is very thin (0–0.05 m). Such a distribution of material along the track was not observed in the field.

Also the temporal distribution of the velocity, with a mean velocity of 13 $cm.min^{-1}$ between 95 and 105 m, during 80% of the run-out time, is not in accordance with the observations.

5 CONCLUSIONS

Run-out distance and time of a small debris-flow could be simulated with a simple numerical dynamic model in which the forces of the equation of motion were resolved using the simple classical Janbu model. It appeared that different sets of combination of c and ϕ- and viscosity values could be found, which match the observed run-out distance and time. However the distribution of material appeared to be more concentrated on flattening slope parts with increasing friction values. A pure cohesive material gives the most regular distribution of material along the track, which was in accordance with the observed distribution. The back calculated cohesion assuming pure cohesive material lies within the range measured in the lab with run-out tests. However the back calculated viscosity is much higher than the laboratory values. It was not possible to create an even distribution of material along the track and a realistic temporal distribution of the travel distance, assuming a pure frictional material ($\phi = 30°$) and a decay of excess pore pressure during run-out.

The simulations show that more information about the rheological characteristics of debris-flow material can be obtained through information about the temporal velocity during run-out and the distribution of sediment along the track.

If the material behaves as a pure cohesive material run-out distance is also dependent on a limiting run-out thickness of the flow. Therefore the initially triggered volume of material, which is spread along the track, determines the run-out distance.

It is also essential to find material indicators, which give a clue to the cohesive and frictional component during the run-out process.

Finally, a great problem is the estimation of the dynamic viscosity of the materials. Dynamic viscosities, obtained from laboratory measurements, seem to be much lower than those back analyzed from field observations.

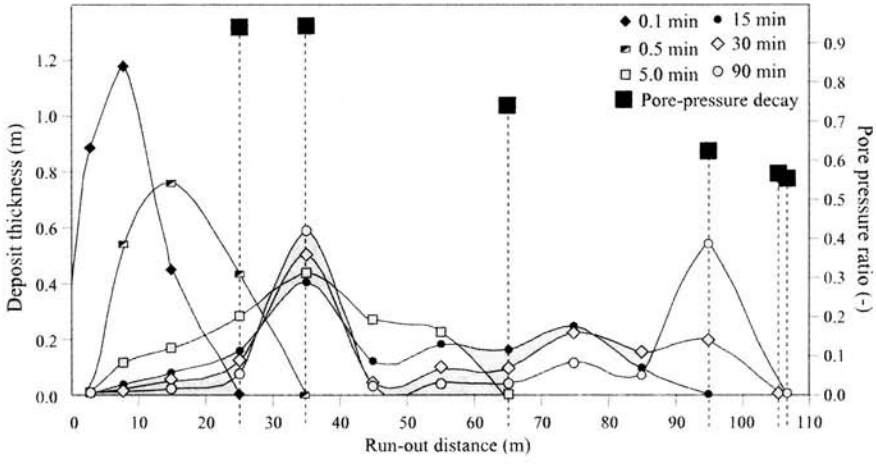

Figure 4. Temporal distribution of the pore pressure ratio p_u in combination with the position of the debris-flow front for scenario 4 (see Table 1).

ACKNOWLEDGMENTS

This work was supported by grants from the French Ministry of Research in the ACI-CatNat contract MOTE (MOdélisation, Transformation, Ecoulement des coulées boueuses dans les marnes) and from the Centre National de la Recherche Scientifique under the INSU-PNRN contract ECLAT (Ecoulement, Contribution de LAves Torrentielles dans les basins versants marneux). Contribution EOST No 2004-001-UMR7516.

REFERENCES

Ancey, C. 2001. Debris-flows and related phenomena. In N.J. Balmforth & A. Provenzale (eds), *Geomorphological Fluid Mechanics*: 528–547. Heidelberg: Springer-Verlag.

Bingham, E.C. 1922. *Fluidity and Plasticity. New*-York: McGraw-Hill.

Coussot, P. 1997. *Mudflow Rheology and Dynamics*. Rotterdam: Balkema.

Duncan, J.M. & Wright, S.G. 1980. The accuracy of equilibrium methods of slope stability analysis. *Engineering Geology* 16: 5–17.

Hungr, O., Morgan, G.C. & Kellerhals, R. 1984. Quantitative analysis of debris torrent hazards for the design of remedial measures. *Canadian Geotechnical Journal* 21: 663–677.

Iverson, R.M. 2003. The debris-flow rheology myth. In D. Rickenmann & C.-L. Chen (eds), *Debris-Flow Hazard Mitigation, Mechanics, Prediction and Assessment, Proc. intern. conf., Davos, 10–15 September 2003*. Rotterdam: Millpress.

Janbu, N. 1954. Application of composite slip surface for stability analysis. In *Proceedings of the European Conference on Stability of Earth Slopes*. Stockholm: Longman.

Johnson, A.M. & Rodine, J.R. 1984. Debris-flow. In D. Brunsden & D.B. Prior, D.B. (eds), *Slope instability*: 257–362. Chichester: Wiley & Sons.

Major, J.J. 2000. Gravity-driven consolidation of granular slurries. Implications for debris-flow deposition and deposit characteristics. *Journal of Sedimentary Research* 70(1): 64–83.

Major, J.J. & Iverson, R.M. 1999. Debris-flow deposition. Effects of pore fluid pressure and friction concentrated at flow margins. *Geological Society of America Bulletin* 111: 1424–1434.

Malet, J.-P. 2003. *Les "glissements de type écoulement" dans les marnes noires des Alpes du Sud. Morphologie, fonctionnement et modélisation hydro-mécanique*. Doctoral Thesis. Strasbourg: University Louis Pasteur.

Malet, J.-P., Remaître, A., Ancey, C., Locat, J., Meunier, M. & Maquaire, O. 2002. Caractérisation rhéologique des coulées de débris et laves torrentielles du basin marneux de Barcelonnette. Premiers résultats. *Rhéologie* 1: 17–25.

Malet, J-P., Locat, J., Remaître, A.J. & Maquaire, O. (in press). Triggering conditions of debris-flows associated to complex earthflows. The case of the Super-Sauze earthflow (South Alps, France). *Geomorphology*, 18p.

Malet, J.-P., Remaître, A., Maquaire, O., Ancey, C. & Locat, J. 2003. Flow susceptibility of heterogeneous marly formations. Implications for torrent hazard control in the Barcelonnette basin (Alpes-de-Haute-Provence, France). In D. Rickenmann & C.-L. Chen (eds), *Debris-Flow Hazard Mitigation, Mechanics, Prediction and Assessment, Proc. intern. conf., Davos, 10–15 September 2003*. Rotterdam: Millpress.

Maquaire, O., Malet, J.-P., Remaître, A., Locat, J., Klotz, S. & Guillon, J. 2003. Instability conditions of marly hillslopes: towards landsliding or gullying? The case of the Barcelonnette Basin, South East France. *Engineering Geology* 70(1–2): 109–130.

Nash, D.F.T. 1987. A comparative review of limit equilibrium methods of stability analysis. In M.G. Anderson & K.S. Richards (eds), *Slope stability, geotechnical engineering and geomorphology:* 11–77. Chichester: Wiley & Sons.

Whitlow, R. 1995. *Basic Soil Mechanics*. Essex: Longman.